Science of the Total Environment 710 (2020) 136425

Contents lists available at ScienceDirect

Science of the Total Environment

journal homepage: www.elsevier.com/locate/scitotenv

Defining the exploitation patterns of groundwater heat pump systems

Alejandro García-Gil [a,b,*], Corinna Abesser [b], Samanta Gasco Cavero [c], Miguel Ángel Marazuela [d], Jesús Mateo Lázaro [e], Enric Vázquez-Suñé [d], Andrew G. Hughes [b], Miguel Mejías Moreno [a]

[a] Geological Survey of Spain (IGME), C/Ríos Rosas 23, 28003 Madrid, Spain
[b] British Geological Survey, Maclean Building, Wallingford, Oxon OX10 8BB, UK
[c] MRC Harwell Institute, Mammalian Genetics Unit, Harwell Campus, Oxfordshire OX11 0RD, UK
[d] GHS, Institute of Environmental Assessment & Water Research (IDAEA), CSIC, Jordi Girona 18-26, 08034 Barcelona, Spain
[e] Department of Earth Sciences, University of Zaragoza, c/Pedro Cerbuna 12, 50009 Zaragoza, Spain

HIGHLIGHTS

- The exploitation regimes of 27 groundwater heat pump systems were examined.
- Exploitation patterns were identified from the cyclicality and cluster analysis.
- Different usage of the systems conditions the hourly and daily cycles.
- Monthly and yearly cycles are affected by the climatization strategy followed.

GRAPHICAL ABSTRACT

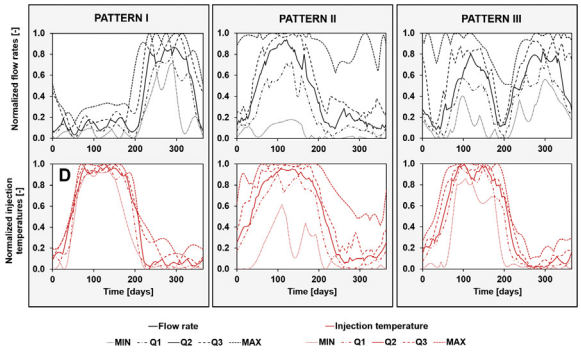

ARTICLE INFO

Article history:
Received 19 November 2019
Received in revised form 28 December 2019
Accepted 28 December 2019
Available online xxxx

Editor: Damia Barcelo

Keywords:
Groundwater heat pump systems
Shallow geothermal energy
Exploitation curve
Renewable energy

ABSTRACT

Shallow geothermal systems are the most efficient and clean technology for the air-conditioning of buildings and constitutes an emergent renewable energy resource in the worldwide market. Undisturbed systems are capable of efficiently exchanging heat with the subsurface and transferring it to human infrastructures, providing the basis for the successful decarbonisation of heating and cooling demands of cities. Unmanaged intensive use of groundwater for thermal purposes as a shallow geothermal energy (SGE) resource in urban environments threatens the resources' renewability and the systems' performance, due to the thermal interferences created by a biased energy demand throughout the year. The exploitation regimes of 27 groundwater heat pump systems from an alluvial aquifer were firstly examined using descriptive statistics. Linear relationships between abstraction and injection temperatures of the systems were assessed by calculating Pearson's *r* correlation coefficient, and used as an evidence of thermal interferences. Then, time series of flow rate, operation temperature and energy transfer were modelled by means of spectral analysis and sinusoidal regression methods, followed by the definition of the relative exploitation patterns. The exploitation regimes examined presented a clear cooling bias and a similar cyclicality. The amplitudes correlated with the different end-user's activities (e.g. medical centres) when high frequency cycles were observed, while climatization strategies (e.g. constant flow rates and modulation of injection temperatures) did so when low frequency cycles were detected. The time series models allowed defining the relative operational pattern of a system and the groups of systems following such patterns. The biases in exploitation regimes of groundwater heat pump systems existing in Mediterranean areas require

* Corresponding author at: Geological Survey of Spain (IGME), C/Ríos Rosas 23, 28003 Madrid, Spain.
E-mail addresses: a.garcia@igme.es, alejgg@bgs.ac.uk (A. García-Gil).

https://doi.org/10.1016/j.scitotenv.2019.136425

correction measures to ensure a more balanced exploitation of the SGE resources. The definition of the characteristic exploitation pattern proposed could be applied to guide resource managers by identifying unbalanced systems, understanding existent exploitation strategies and proposing corrective alternative plans.

1. Introduction

The Paris Agreement (UNFCCC, 2015) established two main objectives to take actions towards combating climate change. The first objective was to keep the rise in average global temperatures below 2 °C, and the second, to limit warming to 1.5 °C in the present century in comparison with pre-industrial levels. Although large economies in the world are increasingly powered by renewable energies up to 33–40% of their total power generation, the global energy system needs to be substantially boosted to meet the Paris Agreement objectives about decarbonisation (IRENA, 2019). Heat accounts for 52% of the total final energy consumption used for building heating and cooling as well as for sanitary water. However, renewable heat consumption in this sector still represents only 10% of the global heat demand (IEA, 2018). Geothermal heat pumps play a relevant role in the decarbonisation of the heating sector since these systems have been classified as the most efficient and cleanest technology for the climatization of buildings (EPA, 1997; Junghans, 2015; Ruhnau et al., 2019). Between 2010 and 2015, the total installed capacity of geothermal heat pumps in the globe increased at a 13.2% annual rate, reaching 50,258 MWt (Lund and Boyd, 2016). This represents 50,258 equivalent installed 1 MWt units, which is the typical capacity value for commercial and public sector systems (Feuvre and Cox, 2009). According to Lund and Boyd (2016), the energy utilization by geothermal heat pumps in 2014 was 326,848 TJ, accounting for energy savings of 194 million barrels of equivalent oil and preventing the release of 82.2 million tonnes of CO_2 to the atmosphere. This tendency is coherent with the H2020 strategy of the European Union (EC, 2010) and its revised directive 2009/28/EC on the promotion of the use of energy from renewable sources, which aims to achieve a 32% share of renewable energy in energy consumption by 2030. Although the technology involved in geothermal heat pumps is generally considered as renewable and environmentally friendly (DiPippo and Renner, 2014), heat transferred to the subsurface generates what is known as heat plumes or thermal affected zones (Lo Russo et al., 2012). Heat plumes have the potential to produce certain thermal interferences (Alcaraz et al., 2016; Galgaro and Cultrera, 2013; Urich et al., 2010) with systems potentially interfering with each other, thus reducing their efficiency; in some cases, to the point where they can no longer be considered as a renewable energy technology (Dû et al., 2015). The high rate of development and use of geothermal heat pumps has to be conducted in a technical, ecological and social way so as to ensure the sustainability of SGE resources (Hähnlein et al., 2013).

There are two main types of geothermal heat pump systems (Self et al., 2013), depending on the technology used to exchange heat with the subsurface. When the heat exchanger is directly introduced in the subsurface by means of a borehole heat exchanger (BHE), the system is named closed loop system or ground-coupled heat pumps (GCHP). The BHE usually consists of a 100 m or deeper borehole where u-pipes or coaxial pipes filled with a circulating heat carrier fluid are introduced and connected directly to a heat pump In the case that a plate heat exchanger is used in the surface to exchange heat with pumped-reinjected groundwater, the system will be known as open loop system or groundwater heat pump (GWHP).

The heat plumes induced by GWHP systems have been studied by means of analytical (Banks, 2011; Pophillat et al., 2018; Rivera et al., 2015) or numerical models (Casasso and Sethi, 2015; Lo Russo et al., 2012; Piga et al., 2017). Using the latter at a city scale (Epting et al., 2017; Garcia-Gil et al., 2014; Herbert et al., 2013; Mueller et al., 2018) has shown the importance of reproducing the thermal regimes of the subsurface for a long-term sustainable management of SGE resources in urban environments. On the other hand, understanding the thermal balance of heating and cooling loads throughout the year has proved to be very sensitive to the dimensions of the heat plumes, thus conditioning the existence of thermal interferences between systems. For this reason, heating and cooling loads have been considered in the definition of a sustainability indicator (García-Gil et al., 2019) and linked to the heat recovery efficiency when the aquifer thermal energy storage (ATES) is considered (Fleuchaus et al., 2019).

Although there exists a comprehensive literature on the thermal response of the aquifers to the operation of GWHP systems, there is a lack of knowledge about the thermal regimes of these systems. The high variability in operation flow rates and discharge temperatures makes it necessary to perform some data treatment to implement these systems into hydrogeological models (Muela Maya et al., 2018). However, the magnitudes and cyclicality of the operation regimes are still investigated in different climate environments to date and they entail one of the key factors triggering the environmental-thermal response of aquifers to SGE exploitation. Therefore, they are of relevance for the thermal management of aquifers in urban areas.

The main objective of this work is to present the results obtained from the examination of 27 GWHP systems exploitation regimes in terms of extraction-injection rates, injection temperatures and energy transfer. To do this, a standardized methodology to analyse the cyclicality of GWHP systems' exploitation regimes is proposed and then operational patterns are defined to evaluate the existing demands and propose their feasible projection as a plausible future SGE resource demand for managing SGE resources. By doing this, a vision of the systems' behaviour in a Mediterranean climate city of Spain will also be given. The results of this paper are of interest to resource managers to understand the systems managed, to study anomalies in the functioning of systems and to estimate future resource demands to adopt pertinent management strategies in general as well as specific measures for individual cases.

2. Data and methods

2.1. Study area

The shallow geothermally-exploited aquifer investigated is located beneath the city of Zaragoza in the Northeastern Spanish autonomous community of Aragón (Fig. 1). Geologically, it belongs to the quaternary alluvial deposits of the Central Ebro Basing and consists of siliceous and carbonate grain-supported gravels in high lateral extension forming tabular bodies with cross-bedding with intercalated sandy lenticular bodies (Luzón et al., 2010). The thickness of the aquifer ranges from 5 to 40 m and is overlaying a sub-horizontal gypsum and marl layers package conforming the aquifer basement. The Ebro River acts as the main natural groundwater drainage system in the studied area conditioning the regional groundwater flow. A piezometric map of the studied area and the general groundwater flow directions are shown in Fig. 1C. On the right margin of the Ebro River, groundwater flows from SW to NE. The Huerva tributary (Fig. 1B) does not affect the general flow pattern of groundwater as it is not hydraulically connected to the aquifer. On the left margin of the Ebro River, the regional groundwater flow pattern (NW-SE) is influenced by the Gállego tributary (Fig. 1B), where the groundwater acquires a NE–SW flow direction. The aquifer transmissivities stand within the range of 3·102 to 4·103 m2 day−1

Please cite this article as: A. García-Gil, C. Abesser, S. Gasco Cavero, et al., Defining the exploitation patterns of groundwater heat pump systems, Science of the Total Environment, https://doi.org/10.1016/j.scitotenv.2019.136425

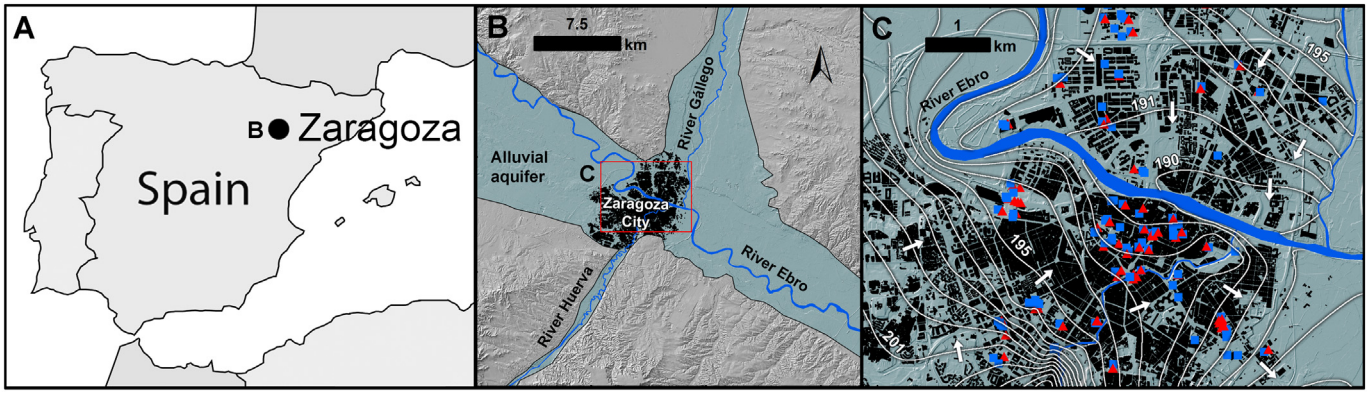

Fig. 1. A) Location of the shallow geothermal exploitation site investigated in the Northeast of Spain. B) Alluvial aquifer extension (light blue) relative to C) the city of Zaragoza. Blue squares and red triangles represent the location of abstraction and injection wells of the existent shallow geothermal systems, respectively. Groundwater head contours are shown in white [m.a.s.l.]. White arrows show groundwater flow directions. (For interpretation of the references to colour in this figure legend, the reader is referred to the web version of this article.)

(CHE, 2010; García-Gil et al., 2015a). Currently, in the city of Zaragoza, 73 GWHP systems are catalogued as exploiting SGE resources of this aquifer by means of 188 water wells, 112 of which are abstraction wells, while 76 are injection wells (Fig. 1). The GWHP systems extracted a total of $24 \cdot 10^6$ m^3 of groundwater in 2010 (Garrido et al., 2012), with $7.4 \cdot 10^6$ m^3 being consumptive. The total installed cooling capacity of these systems is 110 MWt, mainly for cooling purposes, whereas 34 MWt are installed for heating loadings.

2.2. Data acquisition from groundwater heat pump systems

The Spanish geological survey (IGME), in collaboration with the local water authority and GWHP stakeholders in Zaragoza have acquired exploitation datasets of 27 installations between August 2014 and June 2017. These 27 systems comprise 38% of the total number of systems known in the city. The dataset accounts for 1.82 million measurements of pumping/injection flow rates and abstraction/injection temperatures with a 15-minute measurement interval. A detailed list and the main characteristics of GWHP systems considered are given in Table 1. Flow rates were measured using commercial electromagnetic flowmeters equipped with a transmitter that provided data measurements to the centralized control system of each installation. The flowmeters used presented a measuring accuracy of ±0.5% of the actual flow rate. Temperatures were measured using immersion temperature sensors installed in the pipe line before water injection into the aquifer and the data logged was also stored in a centralized control system. Sensing elements used were Pt1000- and Ni1000-passive thermo sensors with a measurement accuracy within the 10–50 °C range of ±0.2 K and ± 0.4 K, respectively.

2.3. Time series analysis

The spontaneous variability in operation regimes of GWHP systems during daily operations and throughout seasons exhibits an oscillatory

Table 1
Main characteristics of monitored groundwater heat pump systems and datasets obtained.

System usage	Label	Number of wells		Active monitoring		Monitored period	Number of measurements	Cluster low freq.	Cluster high freq.	Relative regime pattern
		Out	In	Start	End	[days]				
Administration office space	SGS-AD01	1	1	01-07-14	30-04-17	1035	1,291,680	2	4	II
	SGS-AD02	3	1	01-08-15	23-09-16	419	523,250	2	4	II
	SGS-AD03	3	1	01-01-16	30-04-17	486	606,541	4	4	II
	SGS-AD04	2	1	14-04-15	30-06-17	717	801,216	2	4	III
	SGS-AD05	2	1	02-02-16	01-02-17	366	455,520	3	4	I
	SGS-AD06	1	1	01-05-16	29-04-17	365	455,520	3	4	II
Medical	SGS-MD01	2	1	18-04-16	31-03-17	347	433,602	1	1	I
	SGS-MD02	2	2	01-01-15	30-11-16	700	873,600	4	2	III
Hospital	SGS-MD03	1	1	12-12-14	30-06-17	932	1,163,955	2	4	I
	SGS-MD04	2	1	22-01-16	31-07-17	557	695,123	4	4	II
	SGS-MD05	2	1	01-04-16	28-02-17	334	416,832	4	4	II
Hotel	SGS-HT01	2	1	01-08-15	28-02-17	578	721,318	2	3	II
	SGS-HT02	3	4	01-10-15	30-06-17	639	797,472	2	3	III
	SGS-HT03	2	1	25-06-15	28-02-17	615	767,520	3	3	II
Leisure centre	SGS-PV01	1	1	19-09-15	28-02-17	529	660,205	1	3	III
	SGS-PV02	1	1	02-03-16	28-02-17	362	451,776	1	3	II
	SGS-PV04	2	1	10-10-15	28-02-17	502	625,261	4	–	II
Private office space	SGS-PV03	1	1	04-12-15	27-02-17	451	564,655	1	1	I
	SGS-PV06	3	2	13-01-15	30-06-17	901	1,123,200	3	1	II
	SGS-PV05	1	1	25-05-16	03-07-17	405	505,778	4	1	III
Museum	SGS-MS01	2	1	10-07-15	31-08-17	784	939,419	1	4	II
	SGS-MS02	1	1	13-04-16	30-03-17	352	439,621	2	4	II
	SGS-MS03	1	1	24-03-16	31-05-17	434	541,632	2	4	I
Shopping centre	SGS-SH01	1	1	20-06-15	25-08-16	433	540,384	2	3	III
	SGS-SH02	4	3	01-04-15	30-06-17	822	1,025,856	–	2	III
Sports centre	SGS-SP01	2	1	15-03-16	31-01-17	323	403,611	4	2	III
	SGS-SP02	2	1	05-10-15	28-08-16	328	409,994	1	2	III

Please cite this article as: A. García-Gil, C. Abesser, S. Gasco Cavero, et al., Defining the exploitation patterns of groundwater heat pump systems, Science of the Total Environment, https://doi.org/10.1016/j.scitotenv.2019.136425

behaviour. Such variability is influenced by heating and cooling demands of buildings. Here, it was hypothesized that the different usage of the systems would oscillate following characteristic frequencies. To prove that, total flow rate and injection temperature time series quantifying the power of the different spectral components were evaluated. To infer the structure of the time series, Fourier transform was used, thus decomposing a complex periodic function into a set of periodic basic functions of varying amplitude, period, and phase shift (Kendall and Hyndman, 2007). This method has the advantage of being very well-established and extensively used, as well as to not require educated guesses about the frequency content of the signal, thus obtaining an empirical determination of the full spectrum and physically-intuitive results (Bracewell, 2000; Peters and Williams, 1998). A summary of the most relevant applications to hydrologic problems is provided by Fleming et al. (2002). The time-domain functions taken into consideration were the flow rates $q(t)$ and temperature $T(t)$ time series which were transformed by the forward Fourier transform into frequency-domain signals $G(f)$, where f is the frequency and t is time. The one-dimensional forward Fourier transform for each time-domain function is given by:

$$G(f) = \int_{-\infty}^{\infty} q(t)\, e^{-2\pi i f t}\, dt \tag{1}$$

$$G(f) = \int_{-\infty}^{\infty} T(t)\, e^{-2\pi i f t}\, dt \tag{2}$$

where i is the imaginary unit. The resulting discrete frequency-domain function is given as power spectrum involving the square of amplitude (Dobrin and Savit, 1988) but containing no phase information. The graphical plot of $G(f)$ constitutes the periodogram (Fig. 2A) and the peaks indicate the frequencies that make a significant contribution to the time series measured. Discrete Fourier transform was computed for the 27 GWHP systems (Table 1) using Matlab® (MathWorks, 2012) and a fast Fourier transform (FFT) algorithm based on the FFTW library (Frigo and Johnson, 1998). Both flow rates and injection temperatures were analysed with a discrete time step of 15 min. This sampling resolution might not be the ideal one, since the original signal derived from real systems operations is unknown. The ideal sampling frequency is at least two times the highest frequency of the original signal sampled, according to the Nyquist theorem. Moreover, 15 min sampling would be possibly sparse, particularly because many schemes would have a cycle time closely controlled by the heat pump specification and building demand profile. This means that cycles with a period of minutes will not be considered in this study and hourly cycles should be considered taking into account the sampling limitations shown. To remove extremely low frequency components, trends in the time series were identified using linear regression analysis and outliers were removed from the data prior to transformation. No data windowing was considered necessary.

Since the monitored period covers an average of 545 days, the monthly and yearly periods cannot be analysed properly with FFT authorisms; so, sinusoidal regression analyses were performed using PAST© Software (Hammer et al., 2001). A sum of up to eight unspecified sinusoids with unknown amplitudes and phases were fitted to the daily flow rates and injection temperature time series in order to model their periodicities (Fig. 2B). Daily data used were upscaled following Muela Maya et al. (2018) procedure. The sinusoidal regression algorithm used in PAST© Software is based on a least-squares criterion and singular value decomposition (Press et al., 2007).

Analogous to temperature, the flow rate sinusoidal model $q(t)$ over time t of each GWHP system would be given by the following sum of n cosine functions:

$$q(t) = q_0 + \sum_{i=0}^{n} A_i \cos\left(\frac{2\pi t}{T_i - p_i}\right) \tag{3}$$

where A_i, T_i, and p_i are the amplitude, period, and phase of the i-th cosine function, respectively; and q_0 is the offset flowrate of each GWHP system. The periods were not forced to follow a harmonic proportion and sinusoids were added until the Akaike Information Criterion (AIC) increased.

2.4. Statistical analysis

Basic descriptive statistics were obtained from abstraction and injection temperatures datasets and represented graphically by means of boxplots to provide a general GWHP systems characterization. Descriptive statistics were also calculated for the energy transferred between two consecutive 15-minutal measurements by obtaining the heat power H [W] using 15-minutal measurements of flow rate Q_{15}

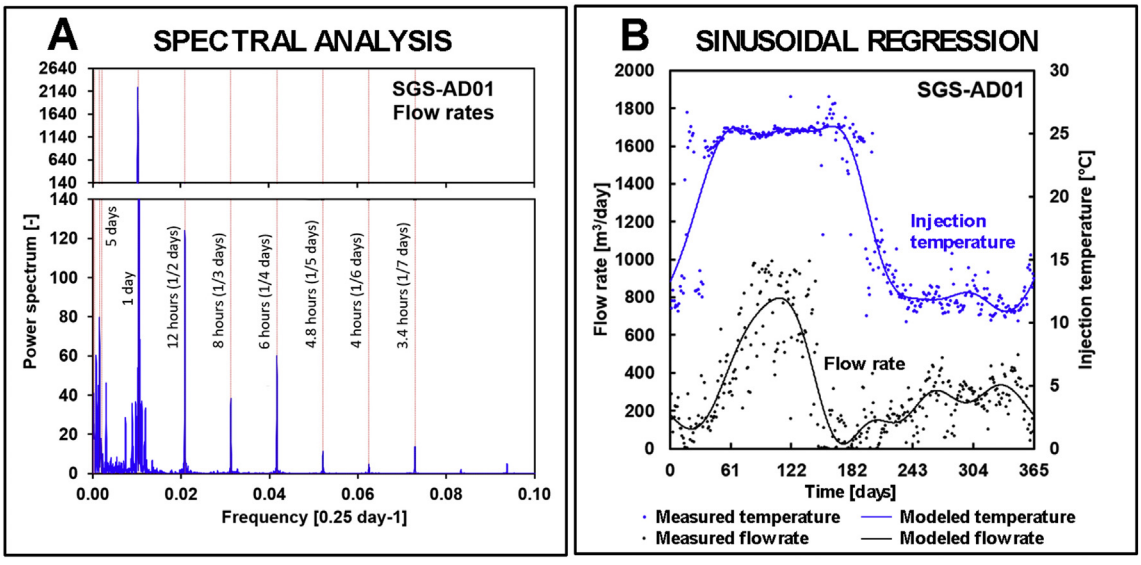

Fig. 2. A) Example of a periodogram of flow rate time series measured for the GWHP system SGS-AD01. B) Example of sinusoidal regression model for flow rate and injection temperature time series measured for the GWHP system SGS-AD01 against punctual daily equivalent measurements.

[$m^3 \cdot s^{-1}$], abstraction temperature T_C [K], and injection temperature T_I [K], following the expression:

$$H = Q\ c_w \rho_w (T_I - T_C) \quad (4)$$

where c_w is the specific heat capacity of water [$J \cdot kg^{-1} \cdot K^{-1}$] and ρ_w is the water density [$kg \cdot m^{-3}$]. Once heat power is obtained, it is multiplied by the 15 min time transferring this power between two consecutive 15-minutal measurements to obtain the heat transferred.

Correlation was used to assess the association strength between abstraction and injection temperatures and their linear relationships. An increase in injection temperatures as a response of increasing abstraction temperatures is here considered as an evidence of intra-system thermal interference (thermal recycling) processes. Normality was verified by using the Kolmogorov-Smirnov (K-S) test. As variables met the assumption of normality, Pearson's *r* coefficients were calculated for all the variable pairs in each GWHP system considered.

After obtaining the amplitudes and power spectrums of the operation cycles identified for each of the 27 GWHP systems considered by using spectral analysis and sinusoidal regression methods, respectively, a clustering analysis was performed to identify groups presenting differences in their exploitation regimes. To potentially identify clusters based on the different usage of each system, a categorical variable related to usage was included in the analysis (Table 1). A two-step cluster analysis was chosen as capable of handling continuous and categorical variables automatically, along with the determination of the optimal number of clusters. Since spectral analysis method was only applied to high frequency cycles (i.e., cycles of 0.15, 0.20, 0.25, 0.33, 0.5, 1, 2, 3, 5 and 7 day periods) and sinusoidal regression method to low frequency cycles (i.e., cycles of 45, 52, 60, 72, 90, 120, 180, and 365 day periods), two cluster analysis were generated for each group of different frequency cycles. Power spectrums and amplitudes of flow rates as well as injection temperatures for such cycles were used as continuous variables. Clustering models fits were firstly validated by the silhouette coefficient, thus ensuring validity of within- and between-cluster distances (Norusis, 2008). The Silhouette coefficient ranges from −1 to +1, where values below 0.3 were assumed to indicate poor quality of the cluster and values equal or above 0.3 indicated a good quality cluster. Secondly, to confirm that the clusters vary significantly across the segmentation variables, mean differences of flow rate and injection temperature amplitudes and power spectrum of the GWHP systems clusters found were evaluated. To do that, one-way ANOVA tests were performed. Normality and sphericity assumptions were corroborated using K-S test and Mauchly's test, respectively (Nahm, 2016). Finally, to confirm the stability of the clusters obtained, datasets were split into random halves and a two-step cluster algorithm was applied again, observing the same number and characteristics in the clusters obtained. The significance threshold for all statistical analysis here described was set at *p*-values under 0.05 (*), with additional and more significant *p*-values of 0.01(**). The data analysis was performed using SPSS 19.0 (IBM, 2010) statistical software.

2.5. Definition of relative exploitation patterns

To compare the relative time distribution of flow rates and injection temperatures of the systems, a definition of the relative characteristic exploitation patterns is proposed here. Since the greater amplitudes were obtained from sinusoidal regression models throughout the year, these models were normalized to their maximum flow rate and injection temperature, respectively. This allowed obtaining a dimensionless variation of daily flow rates and injection temperatures over time so that all installations could be compared and used to identify exploitation patterns within the systems. By comparing the characteristic curves of each GWHP system, three patterns were identified. To characterize those patterns, for each day of the year the minimum, quartiles Q1, Q2 (median) and Q3, and maximum values of the 27 GWHP systems considered were computed and plotted to define the city exploitation patterns identified.

3. Results and discussion

3.1. General GWHP systems characterization

The operation range of GWHP systems in terms of injection and abstraction temperatures is shown in Fig. 3A. During the cooling season, 60% of the installations injected water with a median temperature above 23 °C, while 37% did so above 26 °C. Maximum injection temperatures, excluding outliers, exceeded 35 °C for 26% of the systems, up to a temperature of 41 °C. These injection temperatures have not been reported in previous literature (Haehnlein et al., 2010), indicating that, in the case of this Mediterranean city, the cooling demand requires high injection temperatures. Fig. 3A also shows a positive relationship between absolute injection temperatures ranges during the cooling season and the relative difference between cooling-heating median values of injection temperatures. This is simply due to the fact that injection temperature ranges during heating season are relatively similar and close to the background temperature of the aquifer (17 °C). In Fig. 3B, abstraction temperatures for 93% of the systems are set above the background temperature of the aquifer, thus indicating that groundwater temperatures are not under the natural thermal regime. Abstraction temperatures are 2 °C (i.e. 19 °C) above the background temperatures can be explained by the subsurface urban heat island (SUHI) (Zhu et al., 2011). In this case, 66% of the systems can be considered to be operating on this context. The rest of systems (33%) experienced some type of thermal interference. If the difference between heating and cooling medians is taken into account, four types of systems can be identified. The systems within the first type, named type I and observed for systems SGS-MS03, MD03, AD04, Sh01, AD06, MD01 and PV01, present similar medians, set below 19 °C, for the abstraction temperature found for cooling and heating seasons. This fact is possibly indicating that those systems are not experiencing thermal recycling (intra-system) nor thermal interference from other systems (inter-system), but are influenced by SUHI. Type II systems (observed for SGS-SH02, HT02, MD02, MD05, PV05, PV03, AD03, SP02 and SP01) also present abstraction temperature medians for cooling and heating season below 19 °C but, importantly and contrary to type I systems, these medians are disparate (quantitatively, but not statistically), which could be due to those systems experiencing some thermal recycling within the order of magnitude of SUHI. Type III systems (observed for SGS-MS01, MS02, PV06, AD05 and HT03) presents similar abstraction temperature medians for both cooling and heating season and these values are set above 19 °C, possibly indicating that no thermal recycling occurs but these Type III systems could be influenced by other GWHP system's heat plumes. Type IV systems (observed for SGS-HT01, PV02, AD02, PV04 and MD04) present abstraction temperature median values above 19 °C, but these values are dissimilar between systems for both cooling and heating seasons, potentially showing the presence of thermal recycling and inter-system thermal interference.

Fig. 4 shows the "instantaneous" measurement of energy transfer distribution, highlighting the bias towards cooling for all the systems, except for two of them dedicated exclusively to heat extraction from the aquifer for heating proposes of sport centres SGS-SP01 and SP02. Only 22% of the systems (SGS-P06, MD05, HT02, PV06, AD04 and SH02) present a heating demand in the same order of magnitude as that found for cooling purposes.

3.2. Evidences of thermal-recycling in GWHP systems

The most relevant results obtained from the correlation analysis performed between abstraction and injection temperatures of the systems are shown in Fig. 5. Complete results are provided as supplementary material in Table AI. Considering Pearson's *r* coefficients, *p*-values, the

Please cite this article as: A. García-Gil, C. Abesser, S. Gasco Cavero, et al., Defining the exploitation patterns of groundwater heat pump systems, Science of the Total Environment, https://doi.org/10.1016/j.scitotenv.2019.136425

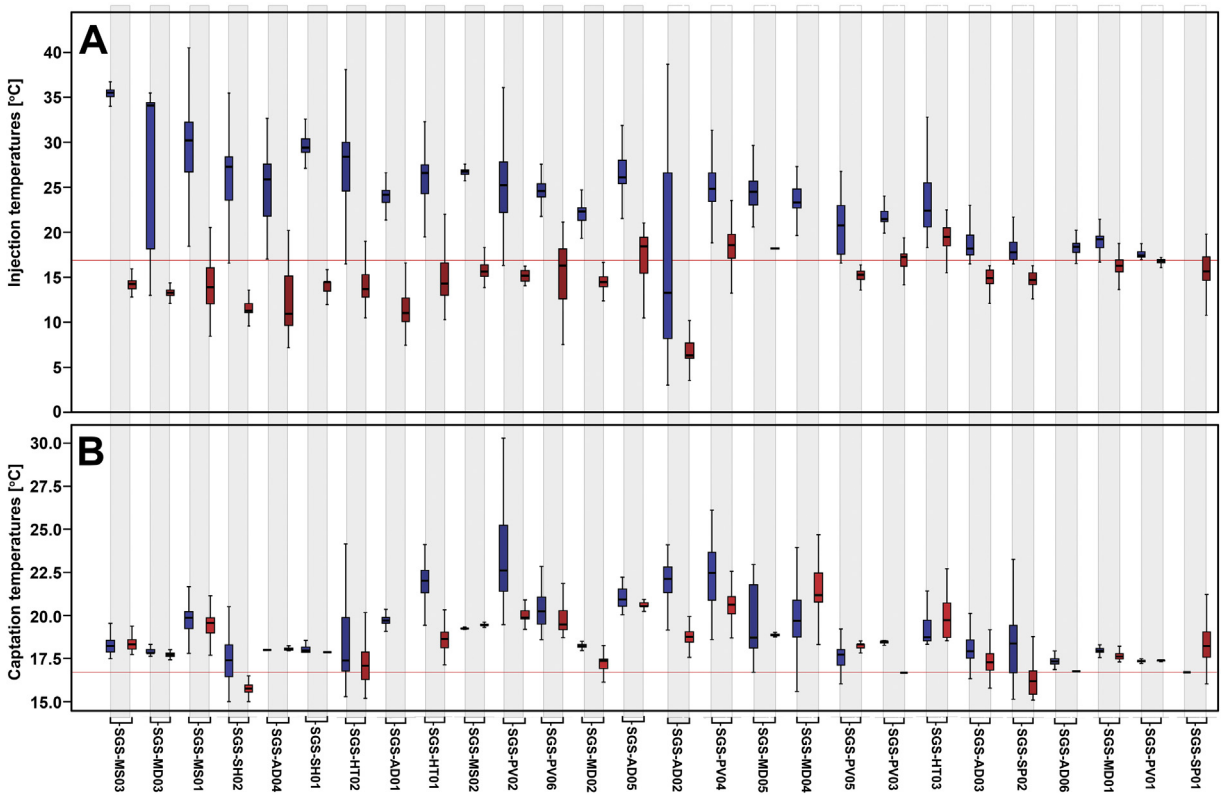

Fig. 3. Boxplots representing the injection (A) and abstraction (B) temperature distribution for each of the 27 GWHP systems (Table 1). Boxplots in blue represent temperatures measured during the cooling season, when the heat transferred to the aquifer is positive. Boxplots in red represent temperatures measured during the heating season, when the heat transferred to the aquifer is negative. Background temperature of the aquifer (17 °C) is denoted by a red line. Outliers have been excluded from the graph. (For interpretation of the references to colour in this figure legend, the reader is referred to the web version of this article.)

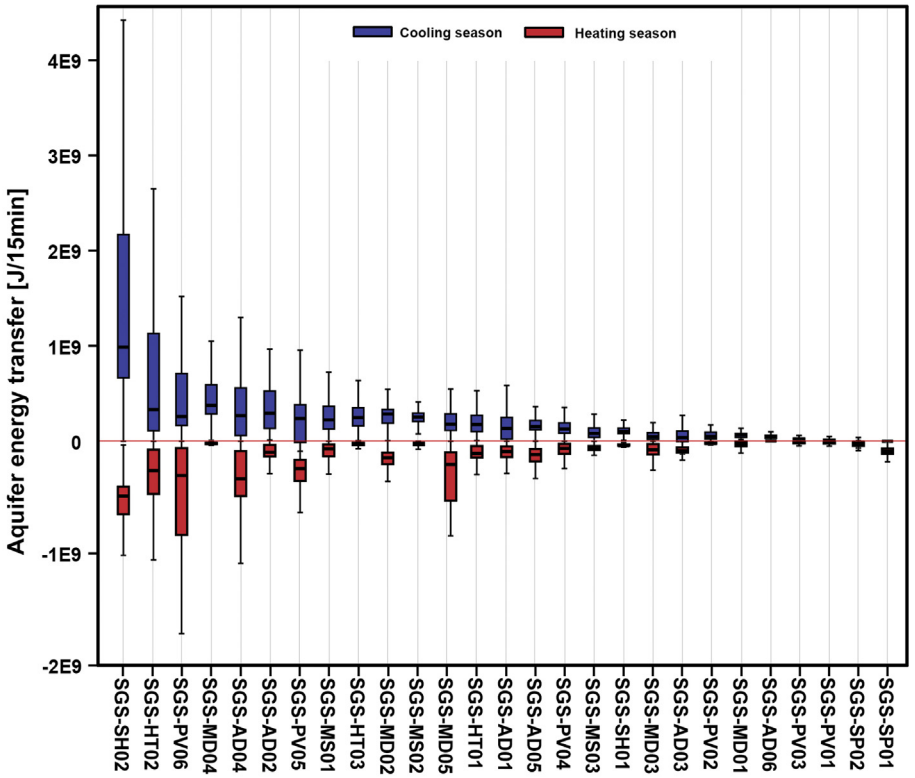

Fig. 4. Boxplots representing the thermal energy transferred from the GWHP systems and calculated from 15-minutal measurements of flow rates and abstraction-injection temperatures. Boxplots in blue represent the thermal energy transferred during the cooling season and boxplots in red represent the thermal energy transferred during the heating season. Outliers have been excluded from the graph. (For interpretation of the references to colour in this figure legend, the reader is referred to the web version of this article.)

Please cite this article as: A. García-Gil, C. Abesser, S. Gasco Cavero, et al., Defining the exploitation patterns of groundwater heat pump systems, Science of the Total Environment, https://doi.org/10.1016/j.scitotenv.2019.136425

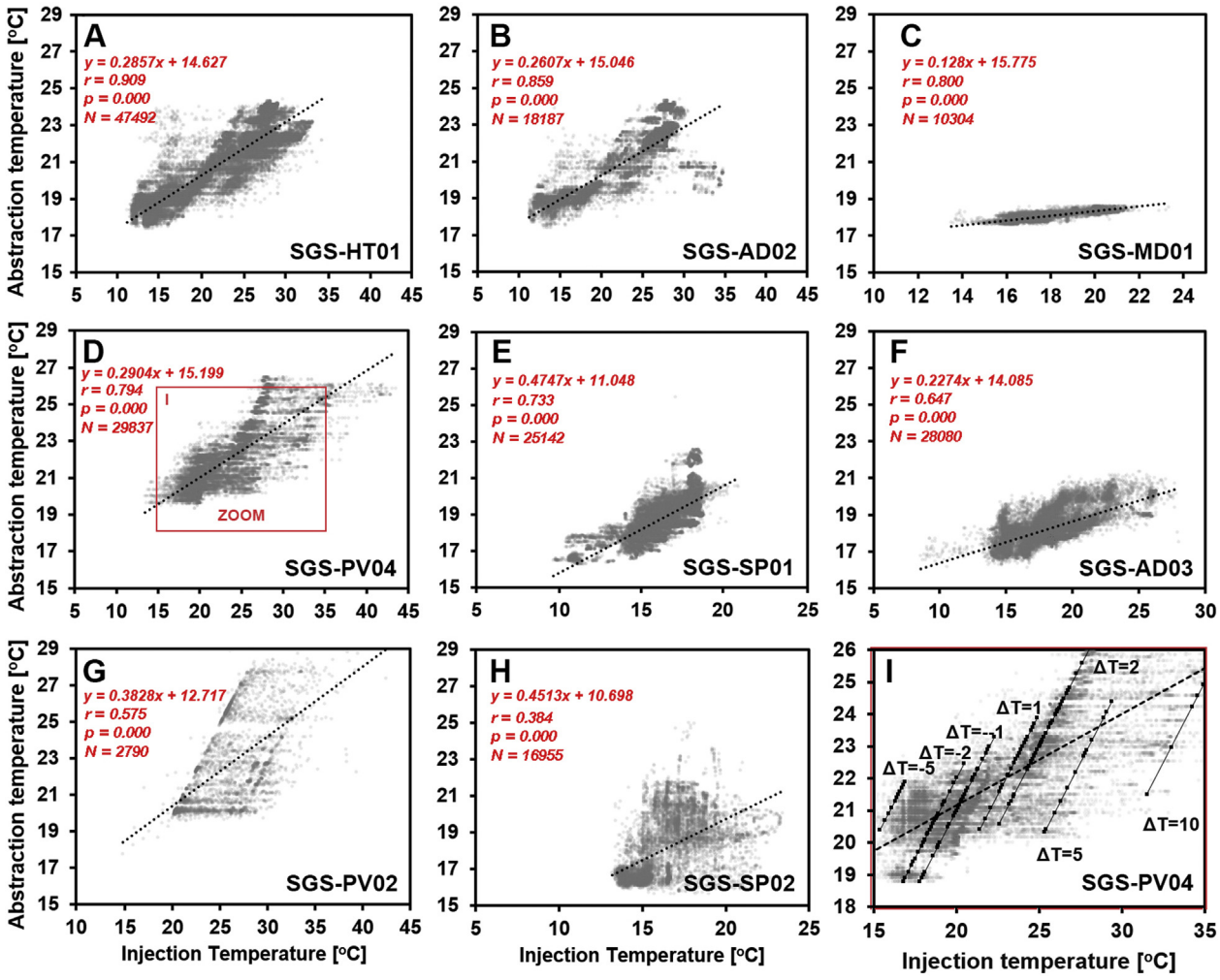

Fig. 5. Results obtained from the correlation analysis performed between abstraction and injection temperatures for eight (A–H) systems. Pearson's r coefficients, *p*-values, high number of measurements used (N) and equations of regression linear models fitted are presented. Secondary linear regression models with slopes values of 1 for installation SGS-PV04 (I) corresponding to a fixed temperature change between abstraction and injection temperatures (ΔT) are also presented.

big sample size for each group and the hydraulics of the problem involved, the results strongly support the strength of the linear relationships found between abstraction and injection temperatures in eight systems. Thermal recycling has a value of 6 °C for SGS-HT01, AD02, PV04, SP01 and SP02 (Fig. 5A, B, D, E and H). The regression linear models showed slopes magnitudes in the range of 0.2 to 0.47 for these systems. SGS-PV02 (Fig. 5G) had a thermal recycling impact of 8 °C, with an intermediate slope in the regression linear model. Systems with smaller slope values of 0.13 and 0.22 (SGS-MD01 and AD03, Fig. 5C and F) also presented lower thermal recycling impacts of 1 and 5 °C, respectively. Although thermal recycling is not only dependent on operational conditions but also on hydrogeological settings (Galgaro and Cultrera, 2013), both users of the installations and local authorities could evaluate the efficiency of the systems by taking into consideration the slope of these linear regression models. The injection-abstraction temperature plots of installations SGS-PV04, HT01, AD02, PV02 also present secondary linear regression models with slopes values of 1 (Fig. 5I). It has been observed that each secondary linear regression model with a fixed temperature change between abstraction and injection (ΔT) was likely a feature of the engineering specification of the heat pump and circulation pumps, which will often involve fixed rates. This indicates that the users condition the exploitation regimes during operation to get to a fixed Δ*T*. When the injection temperature exceeds a given value, the user increases the flow rate with the intention of reducing abstraction temperatures. This automated manoeuvre has a limited effect and the process is repeated as, in global terms, the injection temperature increases in its absolute values in a continuously increasing cooling demand scenario.

3.3. Exploitation cycles identified for GWHP systems

Spectral analysis results (Table 2) showed ten cycles showing relevance for the definition of the exploitation regime at high frequencies for operating flow rates and injection temperatures, within hourly and daily periods. Periodograms obtained for all GWHP systems are provided as supplementary in Fig. AI. The 24 h cycle presents the greater power spectrum and it decreases as a power-law decay as frequency increases. Lower frequency cycles also presented lower power spectrum. The 24 h cycle was present for 93% of the systems in the case of the flow rate variable, and in 96% of the systems for the injection temperature variable. SGS-PV02 is the only system that did not presented any flow rate cycle, denoting very stable non-periodic pumping and injection rates. Flow rates and injection temperature models for low frequency cycles obtained from sinusoidal regression analysis can be found in Table 3. In this case, amplitudes of each cycle identified can be estimated with greater confidence and in appropriate dimensions. The highest amplitudes are found when considering the yearly or the semi-annual cycles. The greatest amplitudes for flow rates cycles is 1420 m^3 day^{-1} (SGS-AD06) and 13.7 °C for the injection temperatures cycles (SGS-MS03). All sinusoidal models for flow rates presented the

Please cite this article as: A. García-Gil, C. Abesser, S. Gasco Cavero, et al., Defining the exploitation patterns of groundwater heat pump systems, Science of the Total Environment, https://doi.org/10.1016/j.scitotenv.2019.136425

Table 2
High frequency spectral analysis results of flow rates and injection temperature for 15-minutal time series of the 27 GWHP systems considered (Table 1). Power spectrum is given for each cycle period when found during the analysis.

Label	Power spectrum of flow rates [−]										Power spectrum of injection temperatures [−]									
	Cycle period [days]										Cycle period [days]									
	0.15	0.20	0.25	0.33	0.50	1.00	2.00	3.00	5.00	7.00	0.15	0.20	0.25	0.33	0.50	1.00	2.00	3.00	5.00	7.00
SGS-AD01	–	9.9	60.0	38.5	124.2	2150.9	–	43.7	–	79.6	30.1	101.8	34.7	19.7	–	1893.1	–	–	–	–
SGS-AD02	17.2	9.7	–	–	80.8	–	45.1	42.2	–	82.4	12.3	16.2	–	20.5	96.4	152.8	68.9	–	–	–
SGS-AD04	16.8	–	63.3	–	22.1	1080.7	76.2	166.8	–	434.0	16.0	–	23.6	29.8	12.7	903.3	60.9	156.9	44.6	374.9
SGS-AD05	23.4	–	120.2	114.3	395.4	1444.2	–	–	–	–	–	–	6.4	11.0	20.9	87.9	–	–	95.9	–
SGS-AD06	10.0	12.3	51.8	67.1	84.5	1881.4	–	235.3	–	596.6	10.9	16.3	34.5	29.7	65.7	929.5	23.6	160.6	26.8	497.9
SGS-AD03	–	16.3	117.8	68.1	289.2	949.9	–	–	–	–	–	10.3	25.0	9.1	112.5	482.1	–	–	15.0	–
SGS-MD03	31.1	17.5	28.5	37.2	84.5	471.6	–	–	–	–	–	–	–	25.7	–	–	–	–	–	–
SGS-MD04	–	14.7	20.0	39.7	15.5	1392.7	–	50.6	–	262.9	–	30.2	–	100.8	–	1245.4	–	20.7	–	87.8
SGS-MD05	–	–	–	–	7.4	289.8	–	–	31.0	103.1	–	–	–	10.7	13.3	2109.4	–	80.2	–	–
SGS-HT01	18.2	11.2	–	–	–	96.5	36.2	–	–	64.3	–	–	–	–	42.7	232.3	13.4	–	24.5	–
SGS-HT02	–	–	–	–	–	9.6	–	–	–	–	–	–	–	–	–	151.4	–	–	11.5	–
SGS-HT03	–	–	–	–	5.2	–	–	–	47.0	46.4	–	5.1	9.5	65.4	88.3	724.9	–	–	69.9	–
SGS-PV01	–	–	–	–	–	–	–	–	–	–	12.7	11.8	–	16.7	23.8	55.2	–	–	–	–
SGS-PV02	–	–	16.1	18.2	56.3	822.1	–	–	–	1128.8	9.8	10.9	25.7	18.7	65.0	659.6	117.9	83.8	–	862.4
SGS-PV04	72.7	50.3	93.9	253.3	80.1	5682.4	–	–	–	234.8	32.5	56.6	28.9	212.7	–	3533.2	–	56.6	–	209.0
SGS-MD01	–	89.6	–	210.1	64.9	2188.7	–	351.5	–	724.2	–	93.1	–	213.4	–	2054.5	49.1	335.0	–	614.1
SGS-MD02	10.9	9.8	23.2	146.0	490.9	409.9	57.0	103.9	–	129.0	8.9	19.1	14.4	118.5	437.8	448.8	55.8	54.6	–	77.1
SGS-MS01	–	7.3	13.2	14.1	46.7	726.9	–	–	57.6	82.4	–	–	–	9.9	13.9	453.0	–	–	13.9	16.1
SGS-MS02	23.4	13.1	39.4	70.8	45.0	1475.9	–	–	–	51.1	22.7	16.5	42.5	76.2	45.2	1608.0	27.4	32.1	–	42.7
SGS-MS03	20.8	9.4	71.2	28.5	81.6	882.0	–	–	–	–	26.9	8.6	90.8	55.8	80.1	1476.6	–	29.0	–	69.0
SGS-PV03	9.2	39.7	72.6	87.5	246.3	815.3	–	–	–	208.6	–	40.9	102.8	116.5	291.5	958.4	–	–	–	225.5
SGS-PV06	–	9.4	37.7	25.2	199.6	2022.8	38.9	393.0	–	1168.1	–	14.9	23.6	48.5	165.1	282.7	–	80.2	35.3	117.4
SGS-PV05	18.8	21.8	–	170.9	111.8	2079.1	–	178.7	–	510.5	20.0	41.2	23.1	184.4	187.4	531.2	–	29.9	–	94.7
SGS-SH01	–	15.3	13.1	–	40.2	316.4	–	–	–	–	21.2	73.1	–	–	319.2	1489.6	–	–	–	–
SGS-SH02	–	18.3	18.0	37.7	255.6	1399.8	–	–	–	–	–	17.5	23.3	–	1512.3	15.2	–	–	–	–
SGS-SP02	37.8	–	26.4	36.1	723.4	554.5	–	–	–	–	31.8	–	16.5	57.0	899.6	669.6	–	–	–	37.3
SGS-SP01	–	7.8	19.7	162.8	145.5	106.8	–	81.9	–	–	19.8	7.9	11.5	113.7	178.4	415.1	–	–	–	–

quarterly (except SGS-MS02), six-monthly and yearly cycles. The same cycles were found for all systems in the case of injection temperature cycles, except for SGS-AD06, which only presented the yearly cycle and a low amplitude of 1.12 °C.

The cluster analysis identified four cluster groups in both low and high frequency cycle groups. The GWHP systems included in each cluster are shown in Table 1. High frequency clusters found had a Silhouette measure of cohesion and separation value of 0.30, thus ensuring a fair

Table 3
Low frequency sinusoidal regression results for flow rates and injection temperature daily time series of the 27 GWHP systems considered (Table 1). Amplitude is given for each cycle period when found during the analysis.

Label	Amplitude of flow rates [m^3/day]								Amplitude of injection temperatures [°C]							
	Cycle period [days]								Cycle period [days]							
	45	52	60	72	90	120	180	365	45	52	60	72	90	120	180	365
SGS-AD01	–	–	19.9	46.2	7.7	111.6	222.6	171.8	–	–	0.32	0.39	0.14	2.13	0.35	8.21
SGS-AD02	–	–	–	–	–	59.5	219.4	389.8	–	–	–	–	0.72	0.44	0.92	6.91
SGS-AD04	–	–	–	105.3	109.1	27.1	353.2	76.0	0.63	0.44	0.66	0.43	0.89	1.47	0.39	9.12
SGS-AD05	–	82.7	185.5	273.6	187.5	131.1	630.7	999.6	–	–	–	–	0.79	0.98	0.90	6.08
SGS-AD06	–	–	–	–	41.7	342.4	818.8	1420.0	–	–	–	–	–	–	–	1.12
SGS-AD03	155.7	157.0	117.3	93.9	154.6	199.8	263.8	525.0	–	–	–	–	–	0.24	0.24	1.64
SGS-MD03	14.4	20.6	9.6	28.5	59.7	42.4	58.3	228.5	–	–	–	0.62	1.26	0.90	3.99	11.50
SGS-MD04	–	–	–	–	–	96.6	315.8	778.6	0.12	0.12	0.15	0.34	0.39	0.34	0.60	1.44
SGS-MD05	–	–	55.3	41.3	66.3	63.5	210.8	549.9	–	–	–	–	0.21	0.35	0.53	3.01
SGS-HT01	65.3	23.4	81.5	23.3	91.8	63.4	242.3	309.7	0.39	0.22	0.57	0.22	0.51	1.33	1.15	7.84
SGS-HT02	31.5	78.2	43.0	74.8	54.0	102.4	387.1	158.6	0.76	0.68	0.37	0.66	1.15	2.31	0.61	11.66
SGS-HT03	–	–	–	–	–	443.9	188.2	891.9	0.25	0.22	0.07	0.72	0.65	0.88	1.30	2.79
SGS-PV01	0.7	0.9	0.7	1.2	0.8	3.0	0.5	4.4	0.03	0.04	0.04	0.05	0.08	0.08	0.01	0.57
SGS-PV02	–	–	–	–	2.1	3.4	14.3	31.1	–	–	–	–	0.10	0.28	0.37	4.30
SGS-PV04	19.2	90.4	114.9	115.8	269.8	219.4	180.5	431.3	–	–	–	–	–	0.39	1.23	5.54
SGS-MD01	15.5	39.5	31.6	27.4	54.8	39.3	68.7	130.5	–	–	–	–	0.28	0.20	0.20	2.00
SGS-MD02	27.9	42.1	98.7	32.3	144.1	172.1	214.2	284.3	–	–	–	0.25	0.55	0.42	1.18	3.99
SGS-MS01	49.5	52.6	79.2	73.3	66.8	90.2	41.8	223.5	0.33	0.83	0.35	0.30	0.49	1.19	0.75	3.90
SGS-MS02	–	–	–	–	–	–	85.6	163.1	–	0.15	0.47	0.51	0.78	1.16	0.60	6.77
SGS-MS03	–	–	7.2	14.1	12.7	10.7	51.7	100.6	1.33	0.43	1.78	1.25	2.13	3.44	2.82	13.36
SGS-PV03	–	–	3.5	5.5	1.9	9.3	22.6	32.5	–	0.28	0.51	0.03	0.63	0.75	1.31	3.82
SGS-PV06	–	–	–	–	104.1	171.0	334.9	1164.0	0.65	0.32	0.14	0.82	1.09	0.68	0.72	3.17
SGS-PV05	–	–	49.9	73.0	53.4	106.1	306.3	225.1	–	0.40	0.56	0.28	0.69	0.34	1.35	3.29
SGS-SH01	–	7.7	3.4	11.4	8.9	19.7	49.1	19.9	0.50	0.71	0.21	1.38	1.91	0.19	4.12	8.69
SGS-SH02	–	–	–	–	117.6	197.6	885.5	275.2	0.28	0.28	0.43	0.54	0.71	2.26	1.28	9.35
SGS-SP02	–	7.1	12.2	9.0	11.5	32.1	63.7	39.9	–	–	0.12	0.13	0.12	0.55	0.35	1.79
SGS-SP01	–	–	15.7	132.1	36.9	199.8	152.6	139.9	–	–	–	–	–	0.32	0.29	1.59

Please cite this article as: A. García-Gil, C. Abesser, S. Gasco Cavero, et al., Defining the exploitation patterns of groundwater heat pump systems, Science of the Total Environment, https://doi.org/10.1016/j.scitotenv.2019.136425

quality for the clusters obtained. The size of the clusters accounted for 15.4, 15.4, 23.1 and 46.2% of the data. A total of seven input variables were used, including system usage as a categorical variable. The main predictor (input variable of importance in the clustering process) was the system usage. Results from the one-way ANOVA analysis for the other 6 predictors used in this cluster analysis are shown in Fig. 6A. The results obtained from both analyses allowed reaching several partial conclusions. Cluster 1, constituted by GWHP systems installed in private office spaces and 50% of medical centres, were characterized by pronounced 8- and 24-hour cycles in relation to flow rates and injection temperatures. Cluster 2 included all the sport centres and 50% of the shopping centres and the rest of the medical centres, and showed relatively important of 8-hour cycles for flow rates and injection temperatures and high importance of 12-hour cycles of flow rates and injection temperatures. Cluster 3 includes all the leisure centres and hotels, and the other half of shopping centres. Those systems are characterized by low power in the spectrum of the cycles, thus indicating a stable flow rate and injection temperature at an hourly and daily scale. Finally, cluster 4 consists of all hospitals, museums and administration office spaces and is characterized by 8- and 12-hour cycles set within the overall mean, with 24-hour cycles being especially relevant.

On the other hand, four low frequency clusters were obtained presenting a Silhouette coefficient of 0.55, thus ensuring the trustworthiness of the cluster. The sizes of the clusters entailed 23.1, 34.6, 15.4 and 26.9% of the data. The main predictors were the annual flow rate cycles, followed by the annual injection temperature cycles and the 4-month and 6-month cycles. Results from the one-way ANOVA analysis of the predictors are shown in Fig. 6B. Cluster 1 includes GWHP systems presenting very stable flow rates and amplitude cycles below the value of the quantile 25. Its injection temperatures throughout the year also present low amplitudes, but still similar to that of clusters 3 and 4. Systems included within cluster 2 also present stable flow rates for all the cycles considered but, in contrast to those within the rest of clusters, present a significantly higher temperature amplitude for the annual cycle. These type of systems seem to respond to heating and cooling demands by maintaining the flow rates along the year and by adapting the injection temperature. Cluster 3 seems to include systems presenting the inverse strategy to that of cluster 2, i.e., adopting injection temperature cycles with low amplitudes in combination with annual, 4-month and 6-month flow rate cycles showing the greatest amplitudes compared to those of other clusters. Cluster 4 is constituted by systems characterized by relative overall median amplitudes for all flow rate cycles and relative low amplitudes for annual injection temperature cycle, similarly to what was found for clusters 1 and 3.

3.4. Relative exploitation patterns identified for GWHP systems

A synthesis of relative time distribution of flow rates and injection temperatures obtained from sinusoidal regression models is presented in Fig. 7. The patterns found and the systems following such patterns are given in Table 1. There were five systems (18%) following pattern I, where low pumping rates were combined with high injection temperatures in the cooling season. Those systems present a low cooling demand due to the usage (sport centres, SGS-SP01 and SP02) or possibly due to the absence of or reduced activity during summer periods. In the heating season, there is an important demand for heating, and pump rates are relatively high with low injection temperatures.

Pattern II was found for 13 systems (48%) and was characterized by both high pumping rates and high injection temperatures in summer, followed by both low pumping rates and low injection temperatures in winter. As expected, this is the most common pattern observed for the 27 GWHP systems studied, since the city of Zaragoza presents a Mediterranean climate with intense summers and soft winters. The last pattern identified, pattern III, was defined by two pumping peaks matching the cooling and heating demand peeks in summer and winter, respectively. A total of 9 systems (33%) presented this pattern, probably related to installations using combined cycle systems. This last pattern is the most sustainable pattern, which tends to reduce bias in heat transfer into the aquifer and prevents overexploitation of SGE resources.

3.5. General outreach in SGE resource management

On the one hand, from a general point of view, the study of cyclicality of the GWHP systems conforms a diagnosis tool for users and managers to identify possible problems or anomalies during operation. Systems experiencing changes in their characteristic cycle frequencies and amplitudes could indicate the existence of operating problems, such as thermal interferences (both intra- and inter-interferences) or clogging processes in the aquifer during water injection operations (Garrido et al., 2016). On the other hand, the approach followed for the study of GWHP systems' thermal regime configures a standardized protocol to identify biases in the exploitation regime of the systems. Although the systems examined are more representative of Mediterranean climates, the methodology proposed could be applied to any other climates in the world. Moreover, possible studies in other climate zones will be of interest to compare the operating cycles and amplitudes throughout the year and at hourly and daily time scale cycles. In addition to understanding operating cycles of GWHP systems all over the world, the methods here proposed allow identifying relative operation patterns of the systems which could be of interest for managing SGE resources in a data-poor context (Stauffer et al., 2013). The definition of relative exploitation patterns could provide a realistic approximation of operation regimes of unmonitored systems possessing limited data, such as yearly water volumes pumped or maximum/minimum injection temperatures. If a general pattern would be described by the user, and knowing the relative exploitation pattern of a homologous system, the injection flow rates and injection temperatures can then be extrapolated. This is especially useful, not only for modeling thermal impacts in the surface (Herbert et al., 2013; Mueller et al., 2018), but for the extrapolation to future SGE resources demands (García-Gil et al., 2015b). This is a necessary step towards the sustainable management of SGE resources in urban environments, where correction measures to ensure a balanced exploitation are required (Epting et al., 2017). Furthermore, the proposed definition of the exploitation patterns could be effectively used by the resource managers as a guide for the identification of unbalanced systems, as well as to understand the big picture of the existent exploitation strategies of the systems managed and to study corrective alternatives/incentives.

4. Conclusions

In this study, an exhaustive assessment of the exploitation regimes of 27 GWHP systems was provided in terms of operational abstraction-injection flow rates and temperatures, by using a 1.82 million measurements dataset. Results from the time series analysis provided a strong evidence for the existence of cyclicality on exploitation regimes of GWHP systems. The obtained results suggest that the different usage for each system conditions the hourly and daily cycles, while the monthly and yearly cycles are affected by the climatization strategy followed. The identification of relative exploitation patterns for the systems has highlighted the existence of three types of systems as an adaptation to the energy demands of each climatization season throughout the year. Abstraction and injection temperatures of eight systems correlated significantly, thus proving the existence of an intra-system thermal interference of up to 8 °C. The methods used in this work have proved suitable for standardizing the definition of a characteristic curve of operation for the systems and for developing future demand models of SGE resources. Resource managers and users will find the results obtained useful for the understanding of climatization strategies based on a combination of stable and/or modulating injection temperatures and/or flow rates. They will also aid in the identification of

Please cite this article as: A. García-Gil, C. Abesser, S. Gasco Cavero, et al., Defining the exploitation patterns of groundwater heat pump systems, Science of the Total Environment, https://doi.org/10.1016/j.scitotenv.2019.136425

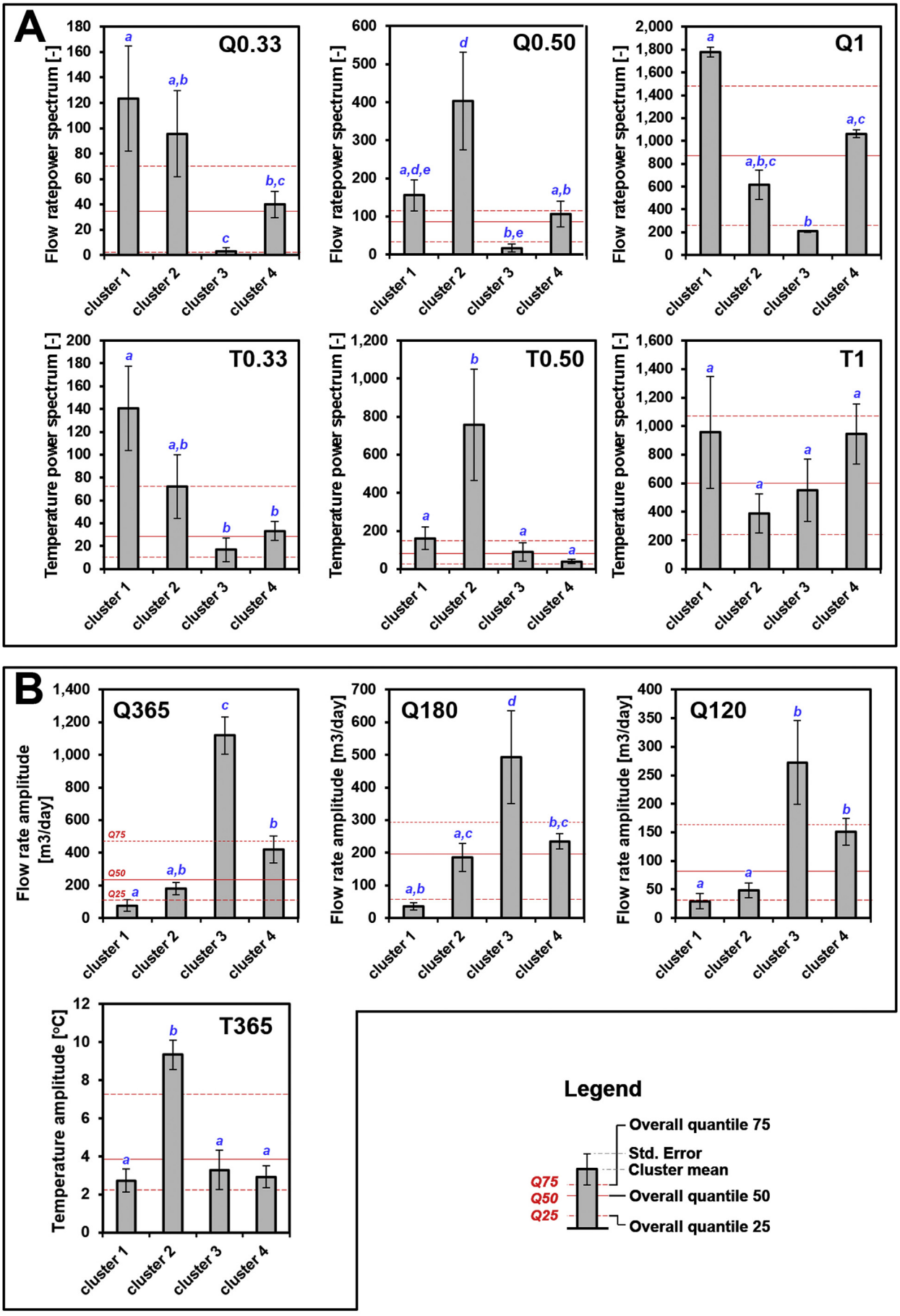
A
Q0.33
Q0.50
Q1
T0.33
T0.50
T1
Flow ratepower spectrum [-]
Temperature power spectrum [-]
cluster 1
cluster 2
cluster 3
cluster 4
B
Q365
Q180
Q120
T365
Flow rate amplitude [m3/day]
Temperature amplitude [ºC]
Q75
Q50
Q25
Legend
Overall quantile 75
Std. Error
Cluster mean
Overall quantile 50
Overall quantile 25

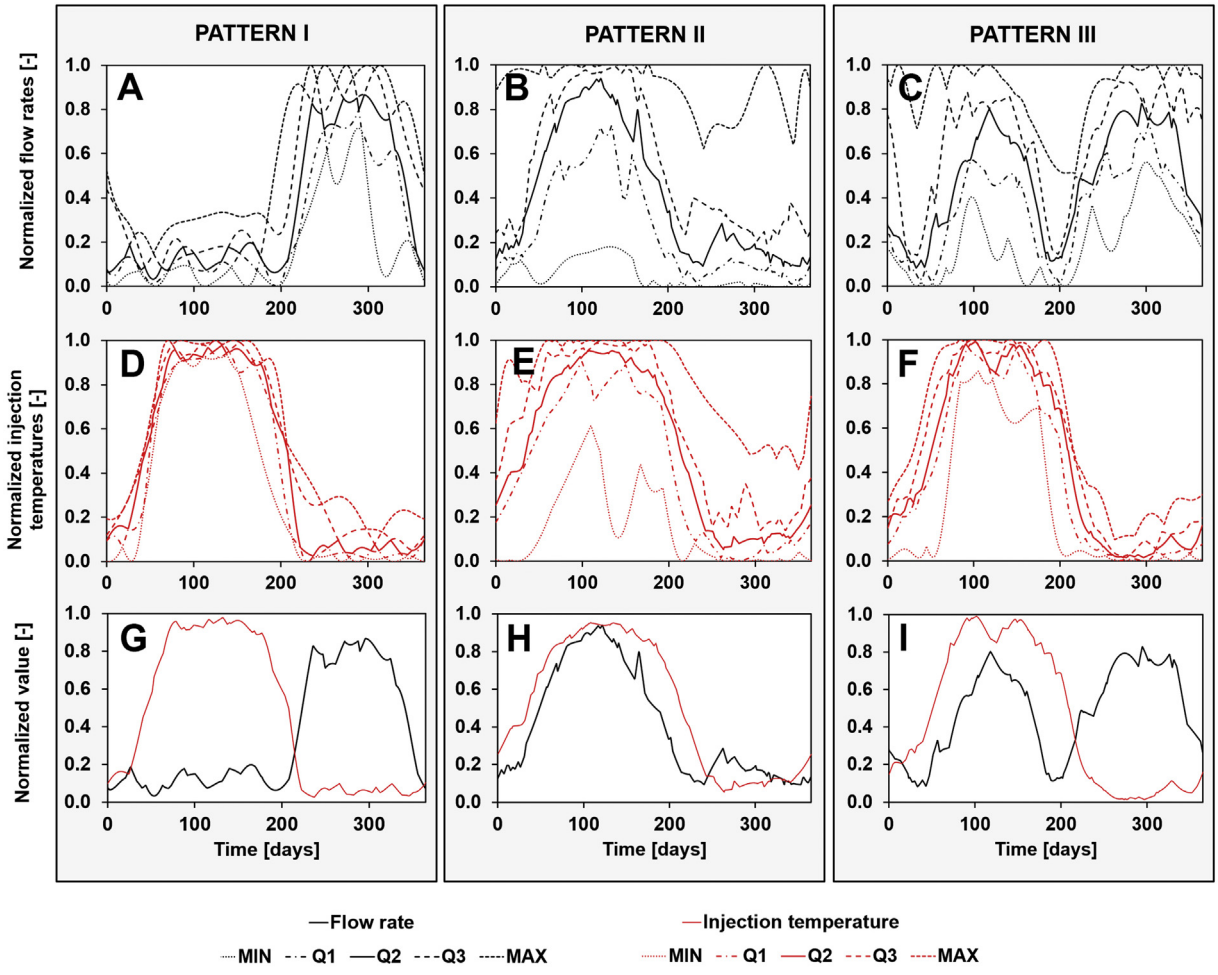

Fig. 7. Relative exploitation patterns identified for GWHP systems. A-C plots represent the normalized flow rates of the 27 systems, reported as minimum (MIN), quantile 25% (Q1), quantile 50% (Q2), quantile 75% (Q3) and maximum (MAX) values. Same nomenclature is shown for normalized injection temperatures in D-F plots. G-I plots present median values (Q2) of the 27 systems for pattern identification. Systems contributing to each pattern are enunciated in Table 1. Time 0 represents 1st of April as the starting point of the cooling season.

unsustainable systems, in the understanding of the existent exploitation regimes in the urban body managed, and in the establishment of corrective initiatives. In the case study investigated (the city of Zaragoza), a cooling bias was identified, as expected for a Mediterranean climate without clear management policies -until the recent years-, which results in the loss of the resources of the aquifer exploited, thus compromising the sustainability of the system, i.e., its SGE renewability as a renewable energy source. To avoid such loss of SGE resources, it is recommended to take action against unbalanced systems, e.g., adopting monitoring and surveillance management measures of the systems and incentivizing equilibrated heating and cooling loads throughout the year. Results obtained from the analyses performed in this work highlights the urgency to adopt correction measures so as to ensure a more balanced exploitation of the SGE resources and justifies the application of the methodologies proposed.

Declaration of competing interest

The authors declare that they have no known competing financial interests or personal relationships that could have appeared to influence the work reported in this paper.

Acknowledgments

The study was supported by the European Community H2020 project MUSE – Managing Urban Shallow geothermal Energy (731166) under the terms of GeoERA programme – ERA-NET Cofund Action.

Appendix A. Supplementary data

Supplementary data to this article can be found online at https://doi.org/10.1016/j.scitotenv.2019.136425.

References

Alcaraz, M., García-Gil, A., Vázquez-Suñé, E., Velasco, V., 2016. Use rights markets for shallow geothermal energy management. Appl. Energy 172, 34–46.
Banks, D., 2011. The application of analytical solutions to the thermal plume from a well doublet ground source heating or cooling scheme. Q. J. Eng. Geol. Hydrogeol. 44, 191–197.
Bracewell, R.N., 2000. The Fourier Transform and its Applications. McGraw Hill.
Casasso, A., Sethi, R., 2015. Modelling thermal recycling occurring in groundwater heat pumps (GWHPs). Renew. Energy 77, 86–93.
CHE, 2010. SITEbro Database. Confederación Hidrográfica del Ebro.

Fig. 6. Results obtained from one-way ANOVA analysis of the predictors used in high frequency (A) and low frequency (B) cycle cluster analyses. Bars represent group means and standard error of the mean (s.e.m.). Bars showing different letters represent a statistical difference between means, while bars with the same letter indicate that no statistical difference was found between those means. T = temperature; Q = flow rate; number beside the letter indicate the period given in days.

DiPippo, R., Renner, J.L., 2014. Chapter 22 - geothermal energy. In: Letcher, T.M. (Ed.), Future Energy, Second edition Elsevier, Boston, pp. 471–492.
Dobrin, M.B., Savit, C.H., 1988. Introduction to Geophysical Prospecting. McGraw-Hill Book Co.
Dû, M.L., Dutil, Y., Rousse, D.R., Paradis, P.L., Groulx, D., 2015. Economic and energy analysis of domestic ground source heat pump systems in four Canadian cities. J. Renewable Sustainable Energy 7, 053113.
EC, 2010. Communication From the Commission. Europe 2020. A Strategy for Smart, Sustainable and Inclusive Growth. European Commission, Brussels.
EPA, 1997. In: Agency, U.S.E.P. (Ed.), Manual on Environmental Issues Related to Geothermal Heat Pump Systems. National Service Center for Environmental Publications, p. 98.
Epting, J., García-Gil, A., Huggenberger, P., Vázquez-Suñe, E., Mueller, M.H., 2017. Development of concepts for the management of thermal resources in urban areas – assessment of transferability from the Basel (Switzerland) and Zaragoza (Spain) case studies. J. Hydrol. 548, 697–715.
Feuvre, P.L., Cox, C.S.J., 2009. In: Directorate, E. (Ed.), Ground Source Heating and Cooling Pumps in England and Wales: State of Play and Future Trends (Environment Agency Report). Environment Agency United Kingdom, p. 81.
Fleming, S.W., Marsh Lavenue, A., Aly, A.H., Adams, A., 2002. Practical applications of spectral analysis to hydrologic time series. Hydrol. Process. 16, 565–574.
Fleuchaus, P., Schüppler, S., Godschalk, B., Bakema, G., Blum, P., 2019. Performance analysis of aquifer thermal energy storage. Renew. Energy 146, 1536–1548.
Frigo, M., Johnson, S.G., 1998. FFTW: an adaptive software architecture for the FFT. Proceedings of the 1998 IEEE International Conference on Acoustics, Speech and Signal Processing, ICASSP '98 (Cat. No.98CH36181). vol. 3, pp. 1381–1384 (vol.3).
Galgaro, A., Cultrera, M., 2013. Thermal short circuit on groundwater heat pump. Appl. Therm. Eng. 57, 107–115.
Garcia-Gil, A., Vazquez-Sune, E., Schneider, E.G., Sanchez-Navarro, J.A., Mateo-Lazaro, J., 2014. The thermal consequences of river-level variations in an urban groundwater body highly affected by groundwater heat pumps. Sci. Total Environ. 485-486, 575–587.
García-Gil, A., Vázquez-Suñé, E., Sánchez-Navarro, J.Á., Mateo Lázaro, J., Alcaraz, M., 2015a. The propagation of complex flood-induced head wavefronts through a heterogeneous alluvial aquifer and its applicability in groundwater flood risk management. J. Hydrol. 527, 402–419.
García-Gil, A., Vázquez-Suñe, E., Schneider, E.G., Sánchez-Navarro, J.Á., Mateo-Lázaro, J., 2015b. Relaxation factor for geothermal use development – criteria for a more fair and sustainable geothermal use of shallow energy resources. Geothermics 56, 128–137.
García-Gil, A., Muela Maya, S., Garrido Schneider, E., Mejías Moreno, M., Vázquez-Suñé, E., Marazuela, M.Á., et al., 2019. Sustainability indicator for the prevention of potential thermal interferences between groundwater heat pump systems in urban aquifers. Renew. Energy 134, 14–24.
Garrido, E., Oroz, M., Coloma, P., Sánchez-Navarro, J., 2012. Transformación de usos y demandas del acuífero urbano de Zaragoza derivado del aprovechamiento geotérmico de sus aguas subterráneas. In: AIH-GE (Ed.), Las Aguas Subterráneas: Desafíos de la Gestión Para el Siglo XXI. International Association of Hydrogeologists, Zaragoza, p. 7.
Garrido, E.A., García-Gil, A., Vázquez-Suñè, E., Sánchez-Navarro, J.Á., 2016. Geochemical impacts of groundwater heat pump systems in an urban alluvial aquifer with evaporitic bedrock. Sci. Total Environ. 544, 354–368.
Haehnlein, S., Bayer, P., Blum, P., 2010. International legal status of the use of shallow geothermal energy. Renew. Sust. Energ. Rev. 14, 2611–2625.
Hähnlein, S., Bayer, P., Ferguson, G., Blum, P., 2013. Sustainability and policy for the thermal use of shallow geothermal energy. Energy Policy 59, 914–925.
Hammer, Ø., Harper, D.A.T., Ryan, P.D., 2001. PAST: paleontological statistics software package for education and data analysis. Palaeontol. Electron. 4, 9.
Herbert, A., Arthur, S., Chillingworth, G., 2013. Thermal modelling of large scale exploitation of ground source energy in urban aquifers as a resource management tool. Appl. Energy 109, 94–103.
IBM C, Armonk (Eds.), 2010. IBM SPSS Statistics for Windows, Version 19.0. IBM Corp, NY.
IEA, 2018. Renewables 2018. 2023 AaFt. Market Report Series. International Energy Agency France, p. 211.
IRENA, 2019. Global Energy Transformation: A Roadmap to 2050 (2019 Edition). International Renewable Energy Agency, Abu Dhabi.
Junghans, L., 2015. Evaluation of the economic and environmental feasibility of heat pump systems in residential buildings, with varying qualities of the building envelope. Renew. Energy 76, 699–705.
Kendall, A.D., Hyndman, D.W., 2007. Examining watershed processes using spectral analysis methods including the scaled-windowed Fourier transform. Subsurface Hydrology: Data Integration for Properties and Processes, pp. 183–200.
Lo Russo, S., Taddia, G., Verda, V., 2012. Development of the thermally affected zone (TAZ) around a groundwater heat pump (GWHP) system: a sensitivity analysis. Geothermics 43, 66–74.
Lund, J.W., Boyd, T.L., 2016. Direct utilization of geothermal energy 2015 worldwide review. Geothermics 60, 66–93.
Luzón, A., Pérez, A., Soriano, M.A., Gil, H., Yuste, A., Pocoví, A., 2010. El relleno de paleodolinas en la cuenca del Ebro y sus posibles aportaciones a la evoluciÛn geodin·mica y ambiental durante el Pleistoceno. Geogaceta Geol. Soc. Spain 48, 11–14.
MathWorks, 2012. MATLAB and Statistics Toolbox Release 2012b. Natick, Massachusetts, United States.
Muela Maya, S., García-Gil, A., Garrido Schneider, E., Mejías Moreno, M., Epting, J., Vázquez-Suñé, E., et al., 2018. An upscaling procedure for the optimal implementation of open-loop geothermal energy systems into hydrogeological models. J. Hydrol. 563, 155–166.
Mueller, M.H., Huggenberger, P., Epting, J., 2018. Combining monitoring and modelling tools as a basis for city-scale concepts for a sustainable thermal management of urban groundwater resources. Sci. Total Environ. 627, 1121–1136.
Nahm, F.S., 2016. Nonparametric statistical tests for the continuous data: the basic concept and the practical use. Korean J. Anesthesiol. 69, 8–14.
Norusis, M.J., 2008. SPSS 16.0 Guide to Data Analysis. 2nd ed. New Jersey.
Peters, T.M., Williams, J.C., 1998. The Fourier Transform in Biomedical Engineering. Birkhäuser Boston.
Piga, B., Casasso, A., Pace, F., Godio, A., Sethi, R., 2017. Thermal impact assessment of groundwater heat pumps (GWHPs): rigorous vs. simplified models. Energies 10, 1385.
Pophillat, W., Attard, G., Bayer, P., Hecht-Méndez, J., Blum, P., 2018. Analytical solutions for predicting thermal plumes of groundwater heat pump systems. Renew. Energy 147 (2), 2696–2707.
Press, W.H., Teukolsky, S.A., Vetterling, W.T., Flannery, B.P., 2007. Numerical Recipes 3rd Edition: The Art of Scientific Computing. Cambridge University Press.
Rivera, J.A., Blum, P., Bayer, P., 2015. Analytical simulation of groundwater flow and land surface effects on thermal plumes of borehole heat exchangers. Appl. Energy 146, 421–433.
Ruhnau, O., Hirth, L., Praktiknjo, A., 2019. Time series of heat demand and heat pump efficiency for energy system modeling. Sci. Data 6, 189.
Self, S.J., Reddy, B.V., Rosen, M.A., 2013. Geothermal heat pump systems: status review and comparison with other heating options. Appl. Energy 101, 341–348.
Stauffer, F., Bayer, P., Blum, P., Giraldo, N.M., Kinzelbach, W., 2013. Thermal Use of Shallow Groundwater. Taylor & Francis.
UNFCCC, 2015. In: Change, FCoC (Ed.), Adoption of the Paris Agreement. Proposal by the President (Draft Decision). United Nations Office, Geneva (Switzerland), p. 32.
Urich, C., Sitzenfrei, R., Möderl, M., Rauch, W., 2010. Einfluss der Siedlungsstruktur auf das thermische Nutzungspotential von oberflächennahen Aquiferen. Österreichische Wasser- und Abfallwirtschaft 62, 113–119.
Zhu, K., Blum, P., Ferguson, G., Balke, K.D., Bayer, P., 2011. The geothermal potential of urban heat islands (vol 5, 044002, 2010). Environ. Res. Lett. 6.

Please cite this article as: A. García-Gil, C. Abesser, S. Gasco Cavero, et al., Defining the exploitation patterns of groundwater heat pump systems, Science of the Total Environment, https://doi.org/10.1016/j.scitotenv.2019.136425